AGU PUBLICATIONS

Geophysical Research Letters

RESEARCH LETTER
10.1002/2015GL064182

Key Points:
- Recent observations of chorus show multiple bands
- Nonlinear wave-particle resonances can occur at subcyclotron frequencies
- Subcyclotron resonance may lead to formation of gaps in banded chorus

Correspondence to:
X. Fu,
xrfu@lanl.gov

Citation:
Fu, X., Z. Guo, C. Dong, and S. P. Gary (2015), Nonlinear subcyclotron resonance as a formation mechanism for gaps in banded chorus, *Geophys. Res. Lett.*, *42*, 3150–3159, doi:10.1002/2015GL064182.

Received 8 APR 2015
Accepted 23 APR 2015
Accepted article online 25 APR 2015
Published online 14 MAY 2015

Nonlinear subcyclotron resonance as a formation mechanism for gaps in banded chorus

Xiangrong Fu[1], Zehua Guo[1], Chuanfei Dong[2], and S. Peter Gary[3]

[1]Los Alamos National Laboratory, Los Alamos, New Mexico, USA, [2]Department of Atmospheric, Oceanic, and Space Sciences, University of Michigan, Ann Arbor, Michigan, USA, [3]Space Science Institute, Boulder, Colorado, USA

Abstract An interesting characteristic of magnetospheric chorus is the presence of a frequency gap at $\omega \simeq 0.5\Omega_e$, where Ω_e is the electron cyclotron angular frequency. Recent chorus observations sometimes show additional gaps near $0.3\Omega_e$ and $0.6\Omega_e$. Here we present a novel nonlinear mechanism for the formation of these gaps using Hamiltonian theory and test particle simulations in a homogeneous, magnetized, collisionless plasma. We find that an oblique whistler wave with frequency at a fraction of the electron cyclotron frequency can resonate with electrons, leading to effective energy exchange between the wave and particles.

1. Introduction

Chorus in the Earth's magnetosphere is a type of whistler wave that has been analyzed for decades using ground-based and satellite observations. Intensive studies have gone into understanding the generation and propagation of these waves and how they affect the magnetospheric plasma [*Sazhin and Hayakawa*, 1992, and references therein]. Chorus is believed to be excited by cyclotron resonance with anisotropic ($T_\perp > T_\parallel$, where $\perp$ and $\parallel$ correspond to directions perpendicular and parallel to the background magnetic field) electrons with energy > 1 keV injected into the inner magnetosphere. Studies have shown that the resonance between chorus and relativistic electrons plays an important role in radiation belt dynamics [*Thorne*, 2010, and references therein]. For example, pitch angle scattering by chorus is a major loss mechanism for trapped electrons in the outer radiation belt. Local acceleration due to interactions between chorus and electrons inside the radiation belt may be a major mechanism for enhanced relativistic electron fluxes [e.g., *Thorne et al.*, 2013].

An important feature of chorus is the presence of a gap at one half the electron cyclotron frequency in its spectrum, separating two frequency bands (therefore called "banded chorus"), a lower band with $0.1 < \omega/\Omega_e < 0.5$ and an upper band with $0.5 < \omega/\Omega_e < 0.8$ [*Meredith et al.*, 2012; *Li et al.*, 2013], where Ω_e is the electron cyclotron angular frequency. Such banded chorus is not unique to the Earth's magnetosphere but is also observed in Saturn's magnetosphere [*Hospodarsky et al.*, 2008]. Recently, using Cluster spacecraft measurements, *Macusova et al.* [2014] reported that sometimes chorus can have more than two bands, with additional gaps near $0.3\Omega_e$ and $0.6\Omega_e$. Most of these "multibanded" chorus events were observed with oblique wave normal angles during disturbed geomagnetic conditions. An example of multibanded chorus observed by Van Allen Probes A on 10 February 2013 is shown in Figure 1.

The narrow gap at $0.5\Omega_e$ between the two bands of chorus has received a lot of attention since it was discovered (for a review of existing theories, see *Sazhin and Hayakawa* [1992] and *Liu et al.* [2011]). *Liu et al.* [2011] hypothesized that two bands of chorus are excited by two different electron populations with temperature anisotropies through linear instability, and the hypothesis has been tested in a case study using Van Allen Probes data by *Fu et al.* [2014]. *Schriver et al.* [2010] explored the possibility of generating the lower band through nonlinear wave-wave coupling of the upper band chorus. *Bell et al.* [2009] assumed that different bands are generated in ducts of either enhanced or depleted cold plasma density. *Omura et al.* [2009] explained the gap at $0.5\Omega_e$, where the group velocity of the whistler wave equals the phase velocity, as nonlinear damping of a slightly oblique whistler wave packet propagating away from the magnetic equator, taking into account the spatial inhomogeneity of the magnetic field. Despite intensive research, a conclusive explanation for banded chorus has not been given yet.

Existing models for banded chorus have only considered the primary (linear) resonances when the resonant particles described by unperturbed orbits see a "time-independent" wavefield. However, it was

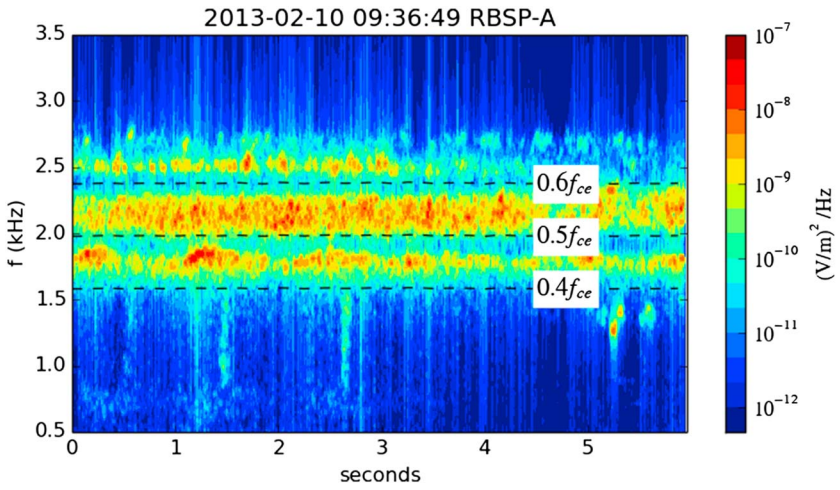

Figure 1. A multibanded chorus measured by Van Allen Probes A on 10 February 2013: the magnetic field spectrogram with two frequency gaps at $0.5f_{ce}$ and $0.6f_{ce}$, where f_{ce} is the local electron gyrofrequency. Black dashed lines indicate $0.4f_{ce}$, $0.5f_{ce}$, and $0.6f_{ce}$, respectively.

recently found that the nonlinear resonances which develop by taking into account the perturbed particle motion in the wavefield can also prompt energy exchange between the wave and particles. For instance, island overlapping due to nonlinear resonances can cause stochastic ion heating in an oblique Alfvén wave with a subcyclotron frequency in the solar corona [*Chen et al.*, 2001; *Guo et al.*, 2008]. Can the nonlinear resonance happen between chorus and electrons? If it can, how will it affect the electrons and chorus? Inspired by the interesting feature of nonlinear resonances at subcyclotron frequencies, we propose the following scenario for the banded chorus observation illustrated in Figure 1. A warm (a few hundred eV), anisotropic ($T_\perp > T_\parallel$) electron velocity distribution drives the whistler anisotropy instability [*Gary et al.*, 2000, 2011], which gives rise to continuous narrowband ($0.4\Omega_e < \omega < 0.7\Omega_e$) enhanced magnetic spectra that appear as a relatively coherent temporal waveform. The cold electron (1–100 eV) response, as will be shown by both theoretical analysis and test particle simulations in this work, demonstrates that there is a nonlinear wave-particle interaction whereby certain electrons come into subharmonic resonance with certain Fourier components. If this interaction transfers energy from the fluctuations to the electrons, the resonant Fourier components will be damped and the fluctuation spectra will develop gaps at $\Omega_e/2$ and other subharmonics as shown in Figure 1.

In this paper, we show that, in the absence of primary resonances, an oblique whistler wave with a frequency at a fraction of Ω_e is able to resonate with the cold electrons nonlinearly, leading to nonlinear damping/growth of the wave with certain electron distributions. This nonlinear mechanism, which involves only wave-particle interactions and works in homogeneous plasmas with a uniform magnetic field, can provide a complementary element to existing theories on chorus. In addition, it can explain additional gaps in chorus spectra around $0.3\Omega_e$ and $0.6\Omega_e$, as reported recently by *Macusova et al.* [2014].

The rest of the paper is organized as follows. In section 2, we present a theoretical framework for analyzing the dynamics of electrons in an oblique whistler wave with uniform background magnetic field. The structures of nonlinear resonances are analyzed using Poincaré maps by solving the equations of motion numerically and confirmed by our theoretical calculations employing the Lie perturbation method. In section 3, we show the results of test particle simulations for an ensemble of electrons with certain velocity distributions. The effects of nonlinear resonances on the electron distribution function and the total kinetic energy are investigated. In section 4, we discuss how this nonlinear mechanism is related to frequency gaps in magnetospheric chorus. Finally, conclusions are given in section 5.

2. Theoretical Analysis

In this section, we analyze the dynamics of electrons in a single oblique whistler wave and a uniform background magnetic field using Hamiltonian theory.

2.1. Hamiltonian

For simplicity, we consider a uniform plasma in a uniform background magnetic field, $\vec{B}_0 = B_0\hat{\mathbf{z}}$, and the whistler wave dispersion relation in the cold plasma limit is given as [*Stix*, 1992, equation (2)–(45)]

$$\left(\frac{ck}{\omega}\right)^2 = 1 - \frac{\omega_e^2}{\omega(\omega - \Omega_e \cos\theta)}, \tag{1}$$

where ω_e is the plasma frequency, k is the wave number, and the whistler wave is oblique with a small wave normal angle θ with respect to the background magnetic field so that $\alpha \equiv \tan\theta = k_x/k_z$. Assuming $\theta \ll 1$ and using the cold plasma theory [*Stix*, 1992], the vector potential can be written as

$$\vec{A} = B_0 x\hat{\mathbf{y}} + \epsilon(B_0/k_z)(\sin\Psi\hat{\mathbf{x}} + \cos\theta\cos\Psi\hat{\mathbf{y}}), \tag{2}$$

where $\Psi = k_x x + k_z z - \omega t$ is the phase of the wave and $\epsilon \equiv B_w/B_0$ denotes the perturbation magnitude. To eliminate electric fields, we move to the wave frame by a transformation, $\vec{x}' = \vec{x} - (\omega/k_z)t\hat{\mathbf{z}}$. Normalizing time to $1/\Omega_e$, magnetic field to B_0, mass to m_e, and length to $1/k_z$, the normalized Hamiltonian for the electron is given by

$$H = \frac{1}{2}\left[p_x^2 + (p_y + x)^2 + p_z^2\right] + \epsilon\left[p_x \sin\psi + (p_y + x)\cos\theta\cos\psi\right] + \frac{1}{2}\epsilon^2(1 - \sin^2\theta\cos^2\psi), \tag{3}$$

where p_x, p_y, and p_z are the canonical momenta and $\psi = \alpha x + z$. In the wave frame, the electron energy is conserved as H does not depend on time explicitly and p_y is a constant of motion since H is independent of y. A set of equations of motion for the electron can be readily obtained from the Hamilton's equation [e.g., *José and Saletan*, 1998]:

$$\dot{x} = p_x + \epsilon\sin\psi, \tag{4}$$

$$\dot{p}_x = -(p_y + x) - \epsilon[\alpha p_x\cos\psi - \alpha(p_y + x)\cos\theta\sin\psi + \cos\theta\cos\psi] - \frac{\epsilon^2}{2}\alpha\sin^2\theta\sin(2\psi), \tag{5}$$

$$\dot{z} = p_z, \text{ and} \tag{6}$$

$$\dot{p}_x = -\epsilon[p_x\cos\psi - (p_y + x)\cos\theta\sin\psi] - \frac{\epsilon^2}{2}\sin^2\theta\sin(2\psi), \tag{7}$$

where dots represent time derivatives.

Without loss of generality, we choose the following parameters relevant to chorus in the Earth's magnetosphere. The whistler wave satisfies $\omega = 0.4\Omega_e$, $k = 0.9\omega_e/c$, and $\theta = 26.6°$ ($\alpha = \tan\theta = 0.5$), where c is the speed of light and $\omega_e/\Omega_e = 5$. So the parallel phase speed of the wave is $\omega/k_z \approx 0.1c$, and the energy is normalized to $m_e(\Omega_e/k_z)^2 \approx 0.06 m_e c^2 = 30.66$ keV. Note that the choice of the whistler wave frequency is for illustration purposes. It will be shown later that, for waves closer to $0.5\Omega_e$, the difference is only in the energy of resonant electrons. The extension to a whistler wave packet with multiple Fourier components is also straightforward [*Lu and Chen*, 2009]. Unless otherwise specified, the above parameters are used in the rest of the paper.

2.2. Poincaré Maps

In our Hamiltonian model, electrons are moving in a four-dimensional phase space (x, p_x, z, and p_z). With Poincaré surfaces of section (or maps), one can visualize the wave-particle resonances in phase space. We construct a Poincaré map in (p_z, z) by recording points when the trajectory of an electron in phase space crosses the surface of $x = 0$ with $p_x > 0$. Electrons are initialized with $x = 0$, $p_y = 0$, fixed H, and a range of parallel velocities p_z's. In Figure 2 (top), a map for electrons with energy $H = 0.3$ is shown in the presence of an oblique whistler wave with $\epsilon = 0.02$. In the map, a major island in (p_z, z) plane located at $p_z = 0$ demonstrates trapping of particles by the wave satisfying $\omega - k_z v_z = 0$ (note $p_z = m_e(v_z - \omega/k_z)$ before normalization), which is the well-known Landau resonance condition. Another set of two islands develops at $p_z = -\frac{1}{2}$, which corresponds to a new resonance condition

$$\omega - k_z v_z = \Omega_e/2, \tag{8}$$

suggesting that electrons can resonate with finite amplitude oblique whistler waves at half cyclotron frequency. A similar mechanism has been proposed for the subcyclotron resonance between ions and oblique Alfvén waves [*Chen et al.*, 2001; *Guo et al.*, 2008]. With higher energy, the primary cyclotron resonance between electrons and the whistler wave can be seen from the island located at $p_z = -1$ (not shown).

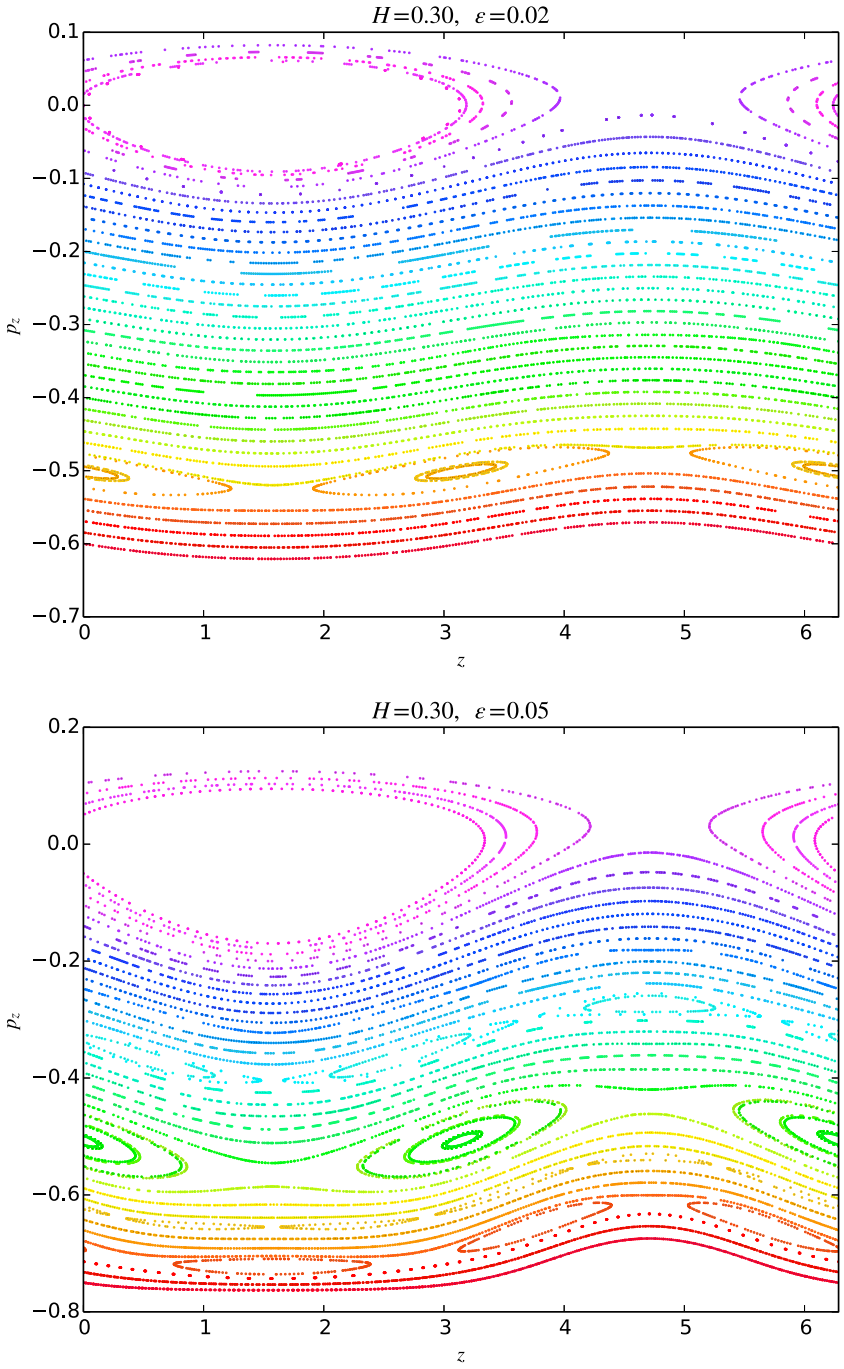

Figure 2. (top) Poincaré map in (p_z, z) plane for electrons in the presence of an oblique whistler wave with an amplitude $B_w/B_0 = 0.02$. The energy of electrons in the wave frame is fixed with $H = 0.3$. Islands develop near $p_z = 0$ and $p_z = -\frac{1}{2}$. (bottom) Similar Poincaré map, but with a larger wave amplitude $B_w/B_0 = 0.05$. Additional resonant islands develop near $p_z = -\frac{1}{3}$ and $p_z = -\frac{2}{3}$.

2.3. Subcyclotron Resonances

We can show that the half cyclotron resonance is the result of nonlinear dynamics by taking into account the perturbed electron orbit in the presence of wavefields. The analysis is greatly simplified in the so-called guiding center coordinates. Through a canonical transformation [*Guo et al.*, 2008], the Hamiltonian becomes

$$H = H_0 + \epsilon H_1 + \epsilon^2 H_2, \tag{9}$$

where $H_0 = J + p_z^2/2$ is the unperturbed guiding center Hamiltonian,

$$H_1 = \sqrt{2J}\left[\cos\phi\sin(\alpha\sqrt{2J}\sin\phi + z) + \sin\phi\cos\theta\cos(\alpha\sqrt{2J}\sin\phi + z)\right], \text{and} \tag{10}$$

$$H_2 = -\frac{1}{2}\sin^2\theta\cos^2(\alpha\sqrt{2J}\sin\phi + z). \tag{11}$$

Here $J = [(p_y+x)^2+p_x^2]/2$ denotes the perpendicular energy and ϕ the gyroangle. Interestingly, if the whistler wave is purely parallel to the background magnetic field ($\theta = 0$), H_2 vanishes and $H_1 = \sqrt{2J}\sin(z-\phi)$ contains only the primary resonance. So the electron dynamics becomes integrable, and there will not be any nonlinear resonance. Due to the dependence of the perturbed Hamiltonian on ϕ and z, both J and p_z vary in time. These variations are related to the magnetic drift of the guiding center which can then give rise to nonlinear resonances via the $\vec{k}_\perp \cdot \vec{X}_g$ term with $\vec{X}_g$ being the magnetic drift.

To analyze the perturbed Hamiltonian, we introduce the Lie transform method [e.g., *José and Saletan*, 1998] which utilizes particular canonical transformations to obtain perturbation series in terms of Poisson brackets. Similar to the approach in *Guo et al.* [2008], a generating function

$$W_1(\phi, z, J, p_z) = \sqrt{2J}\sum_n\left(\sin^2\frac{\theta}{2}J_{n+1} + \cos^2\frac{\theta}{2}J_{n-1}\right)\frac{\cos(n\phi+z)}{n+p_z}, \tag{12}$$

is obtained to remove the first-order perturbations by setting $[W_1, H_0] + H_1 = 0$ with $[\,,\,]$ being the Poisson bracket. This generating function indicates singularities when $p_z = -n$, with n being any integer. In the laboratory frame, they simply correspond to the well-known cyclotron resonance condition $\omega - k_z v_z - n\Omega_e = 0$ when $n \neq 0$ and the Landau resonance condition $\omega - k_z v_z = 0$ when $n = 0$.

After the Lie transformation, the new Hamiltonian becomes $H' = H_0 + \epsilon^2(H_2 + [W_1, H_1]/2) + O(\epsilon^3)$, where the second-order perturbation reads

$$H_2' = \frac{1}{4}\left[\sum_{m,n}(A_{m,n} - \sin^2\theta J_m J_n)\cos(l\phi + 2z) - \sum_{m,n}(B_{m,n} + \sin^2\theta J_m J_n)\cos(m-n)\phi\right], \tag{13}$$

with $l = m + n$. The functions $A_{m,n}(J, p_z)$ and $B_{m,n}(J, p_z)$ are introduced for simplicity. Their explicit expressions are tediously long and will be presented later in a separate paper. The new Hamiltonian clearly shows the existence of nonlinear resonances when the phase $(l\phi+2z)$ remains a constant or $p_z = -l/2$. In the laboratory frame, they correspond to the second-order resonance conditions $\omega - k_z v_z - (l/2)\Omega_e = 0$. The second term in equation (13) does not contribute to resonances. Therefore, our analytical calculation confirms the existence of the nonlinear resonance at the half cyclotron frequency ($l = 1$). Following the result in *Guo et al.* [2008], we know that the island width of second-order resonances is proportional to ϵ while it is $\sqrt{\epsilon}$ for the primary resonances. This means the damping due to second-order resonance is weaker than the primary resonance by square root of the wave magnitude. Continuing to the third-order expansion, we will obtain resonances at $p_z = -l/3$ which is present in Figure 2 (bottom) when the wave has a larger amplitude.

3. Test Particle Simulations

A wave-particle resonance causes efficient energy exchange between the wave and resonant particles. For example, a wave is damped via Landau resonance, while the resonant particles gain same amount of kinetic energy the wave loses. To further illustrate how the nonlinear resonance, at $\omega - k_z v_z - \Omega_e/2 = 0$, can damp waves around the half cyclotron frequency, we perform test particle simulations of a large number of electrons and investigate the changes in the electron distribution and their kinetic energy in the presence of an oblique whistler wave.

In our test particle simulation, about 10^6 electrons with Maxwellian velocity distribution in the lab frame,

$$f(v_x, v_y, v_z) = f_0\exp\left[-m_e\left(\frac{v_x^2+v_y^2}{2T_\perp} + \frac{v_z^2}{2T_\parallel}\right)\right], \tag{14}$$

are loaded initially. Here we choose electron temperatures $T_\perp = T_\parallel \sim 300$ eV so that $v_t = \sqrt{T_\parallel/m_e} \approx |(\omega - \Omega_e/2)/k_\parallel|$. Electrons are advanced according to equations of motion given by equations (4)–(7). In the presence of an oblique whistler wave with wave amplitude $B_w/B_0 = 0.02$, the energy (calculated in the lab frame)

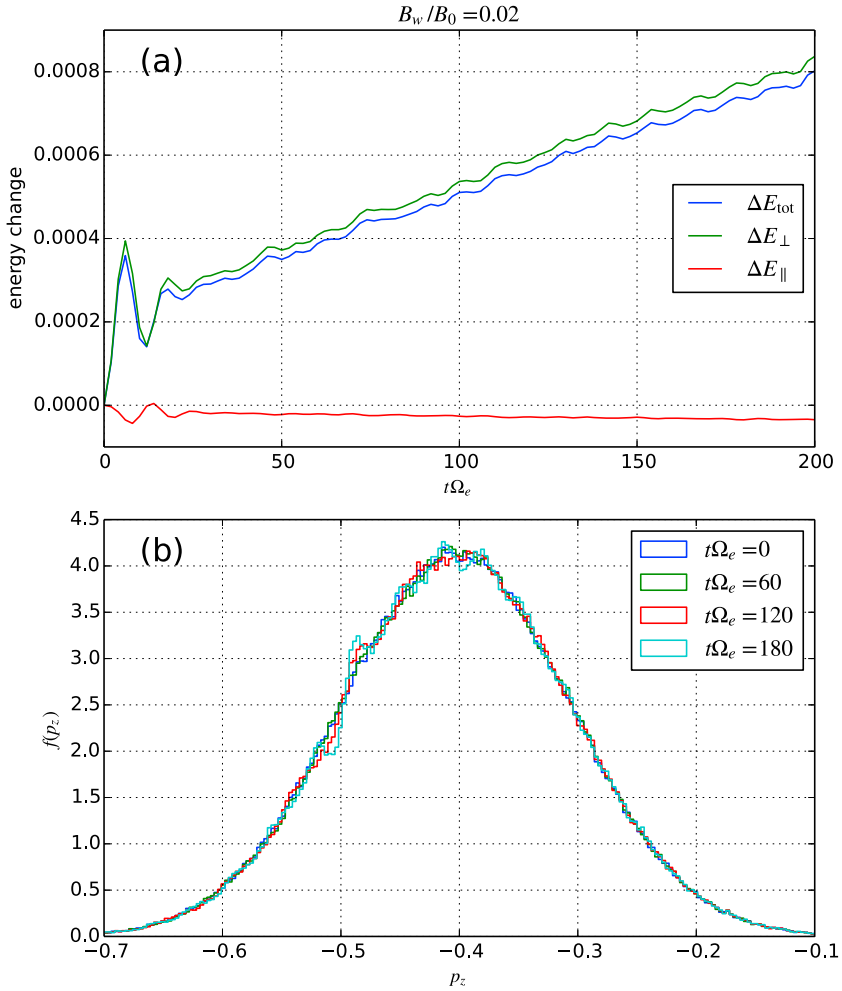

Figure 3. (a) Change of the averaged energies per test electron in the presence of an oblique whistler wave with an amplitude $B_w/B_0 = 0.02$. The averaged initial total energy per electron $E_{tot,0} = 0.028$. (b) The distribution function $f(p_z)$ at different times of the simulation. Changes of $f(p_x)$ and $f(p_y)$ are minor.

evolution of these electrons is shown in Figure 3a. After initial oscillations, the averaged energy per electron (E) increases at a rate $\Delta E/(E_0\Delta t) \approx 10^{-4}\Omega_e$ (where E_0 is the averaged initial energy per electron) and the energy gain is predominantly in the perpendicular direction. In a self-consistent simulation where the wavefield follows Maxwell's equations and the total energy of the system is conserved, the increase of the electron energy must come from the decrease of wave energy. This implies that the wave will be damped by the nonlinearly resonant electrons. The rate of particle energy gain normalized to the wave energy is $2\mu_0 n_e m_e(\Omega_e/k_z)^2\Delta E/(B_w^2\Delta t) \approx 0.02\Omega_e$.

The electron velocity distributions in the wave frame at $t\Omega_e = 0, 60, 120$, and 180 are shown in Figure 3b. Clearly, the parallel velocity distribution $f(p_z)$ deviates from the initial Maxwellian in the vicinity of $p_z = -0.5$, which corresponds to the second-order resonance shown in the Poincaré map in Figure 2. The changes in both $f(p_x)$ and $f(p_y)$ are small (not shown). For the given Maxwellian distribution function, the nonlinear subcyclotron damping steepens the gradient of $f(p_z)$ around $p_z = -0.5$, causing the parallel kinetic energy to decrease, and the perpendicular kinetic energy to increase (see Figures 3a). This is similar to the primary cyclotron resonance where the electrons are scattered along the constant energy surfaces in the wave frame as pointed out by *Kennel and Engelmann* [1966].

Just like the Landau or cyclotron resonance, the nonlinear resonances can lead to damping/growth of the waves at subcyclotron frequencies when the electron distribution satisfies certain conditions (the stability criteria). Even though the particle motion is described as periodic in our theoretical analysis and test particle

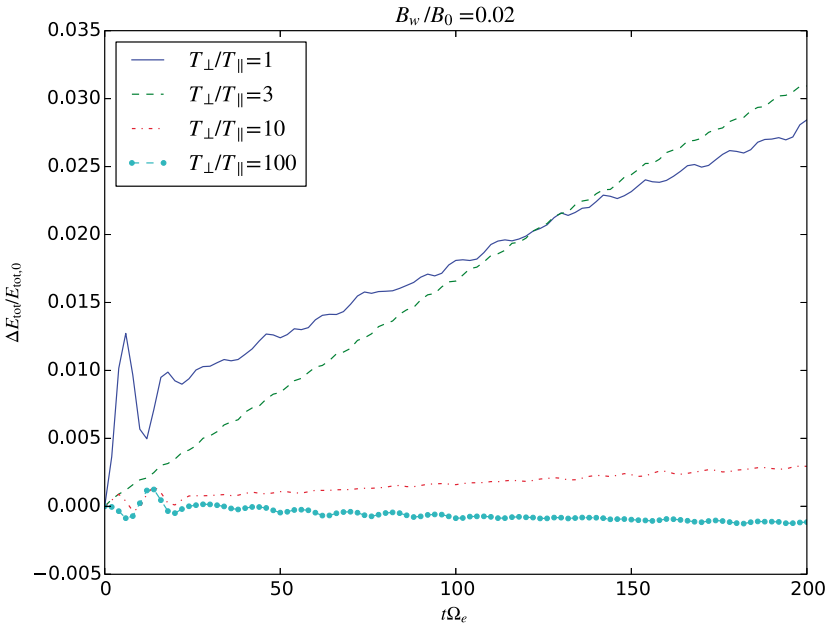

Figure 4. Relative change of energies per electron for cases with temperature anisotropy $T_\perp/T_\parallel = 1, 3, 10,$ and 100. All parameters except $T_\perp$ are fixed.

simulations, what determines the wave damping/growth rate is how fast the resonant particles can take (give) energy from (to) the perturbed fields. This is the same as in Landau or cyclotron damping, which requires the resonant particles to gain energy at a rate faster than their bounce frequency in the perturbed field. The wave begins to saturate when this condition is violated. The difference in the nonlinear damping mechanism is that the relevant bounce motion is now described by the second-order perturbed Hamiltonian and thus becomes much slower than the linear bounce motion. A test particle simulation describes the particle dynamics at the beginning stage of the wave-particle interaction and can predict the rate of energy gain or loss by resonant particles depending on the distributions, as discussed in the following.

When the temperature anisotropy $T_\perp/T_\parallel$ is strong enough, the nonlinear resonance may also lead to decrease of the particle energy and thus instability of the whistler wave. This is demonstrated by a comparison of runs with different initial anisotropies, as shown in Figure 4. Same parameters as those in Figure 3 except the perpendicular temperature are used in these runs. For $T_\perp/T_\parallel = 100$, the electrons lose energy, which implies wave growth in a self-consistent situation. Interestingly, for anisotropies well below the instability threshold, the temperature anisotropy can enhance the nonlinear wave-particle resonance, as shown by the case with $T_\perp/T_\parallel = 3$ initially. This is consistent with our analysis as in equation (12) where a factor of $\sqrt{2J}$ shows the dependence on the particle perpendicular energy.

To further illustrate the subcyclotron resonance and clarify that the energy gain of electrons is not dominated by numerical heating or pseudoheating [*Dong and Singh*, 2013] in our simulations, we carry out two comparison test cases. In the first case, we artificially load electrons with $f(p_z)$ flat in the range $-0.6 < p_z < -0.4$ as shown in Figure 5a. Due to the nonlinear resonance near half cyclotron frequency, electrons gain energy from the wave. In the second case, we remove the resonant particles within $-0.55 < p_z < -0.45$ from the distribution as shown in Figure 5b. The resulting energy gain in the lab frame (Figure 5c) is significantly reduced. Therefore, it is clear that the dominant energy gain of electrons is caused by the nonlinear resonance.

4. Application to Banded Chorus

In the Earth's magnetosphere, cold plasmaspheric electrons (~ 1 eV) extend into a region called the "plasma trough" with $L = 4$–8 (L is the equatorial distance of a magnetic field line from the center of the Earth in the unit of Earth's radius) [e.g., *Carpenter and Anderson*, 1992], where they meet ~ 1 keV electrons from the plasma sheet. Banded chorus is frequently observed in this region [e.g., *Meredith et al.*, 2012]. We conjecture that the gap of the banded chorus may be caused by the nonlinear damping of oblique whistler waves by these cold

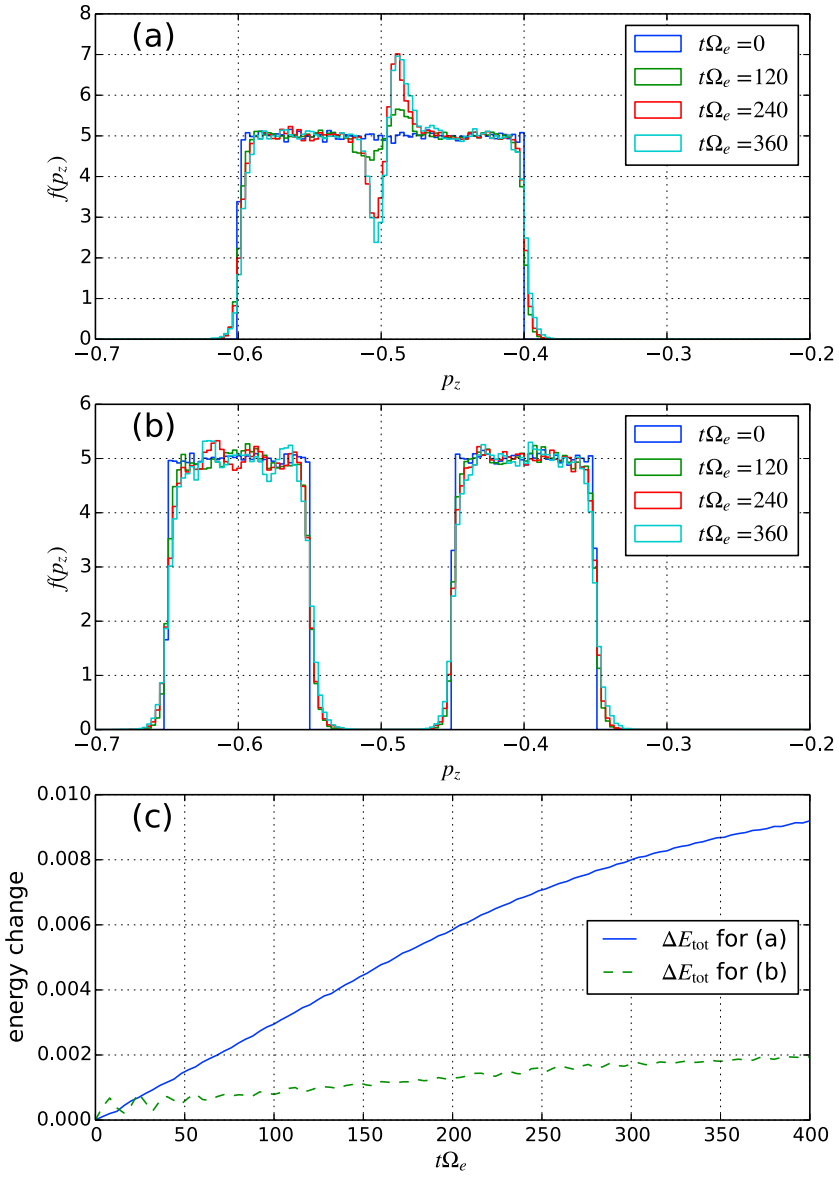

Figure 5. The evolution of the distribution function $f(p_z)$ for (a) an initial flat-top distribution and (b) a flat-top distribution with resonant particles removed. (c) The comparison of the change of total energy per electron is shown.

electrons with energy 1–100 eV. For 10 eV electrons, whose thermal velocity $v_t \sim 6 \times 10^{-3}c$, the nonlinear resonance condition (equation (8)) becomes $\omega \approx 0.5\Omega_e$; i.e., these electrons could damp oblique whistler waves with frequency near $0.5\Omega_e$, leaving a gap in the wave power spectrum.

Wave analysis often shows chorus is quasi-parallel, but we have already shown that even with a wave normal angle of 26.6°, nonlinear wave-particle interactions can be significant. Furthermore, even if the chorus is excited purely parallel in the source region close to the magnetic equator, as the wave propagates away from the equator, it will soon have an oblique component due to the curved nature of Earth's dipole-like magnetic field.

Here we have presented cases with a modest wave amplitude $B_w/B_0 = 0.02$ to better illustrate the nonlinear resonance mechanism with less computational constrains. The numerical integration scheme can introduce errors into the particle's energy; therefore, for smaller wave amplitudes, we need to both reduce the time step to suppress the numerical heating and increase number of particles to resolve the resonance structure in phase space. Typical amplitude of chorus in the magnetosphere is about $B_w/B_0 \sim 0.001$, but large-amplitude whistler waves have also been reported with $B_w/B_0 > 0.01$ [e.g., *Santolík et al.*, 2014]. The subcyclotron

resonance can be strong and effective in damping these large-amplitude whistler waves as shown in the previous section. For smaller wave amplitude, we have also carried out test particle simulations with $B_w/B_0 = 0.002$, $\omega = 0.46\Omega_e$, $T_\parallel = 50$ eV, and $T_\perp = 100$ eV. The results (not shown here) indicate that the same nonlinear resonance occurs, although the rate of the electron energy gain is reduced ($\Delta E/(E\Delta t) \approx 6 \times 10^{-6}\Omega_e$) due to the lower wave amplitude. Therefore, the proposed nonlinear damping mechanism at subcyclotron frequencies is robust and can play a role for waves observed in the magnetosphere. Furthermore, in the presence of multiple whistler modes (or a narrow band) near half cyclotron frequency, the nonlinear damping is expected to be enhanced due to the overlapping of resonances as suggested by *Chen et al.* [2001] and *Lu and Chen* [2009]. This effect will be addressed in a separate paper.

If the wave amplitude increases to $B_w/B_0 = 0.05$, additional resonant islands near $p_z = -1/3$ and $p_z = -2/3$ develop in the Poincaré map (Figure 2, bottom), which may explain the additional gaps near $0.3\Omega_e$ and $0.6\Omega_e$ observed by *Macusova et al.* [2014]. As *Macusova et al.* [2014] reported, multibanded chorus were observed during more disturbed times with the average $Kp \sim 3$, larger than the average $Kp \sim 2$ for chorus observed with one or two bands. These higher-order nonlinear resonances, as well as the half cyclotron resonance we have shown, belong to a set of nonlinear resonant conditions below the cyclotron frequency, $\omega - k_\parallel v_\parallel = N\Omega_e/M$, where M, N are integer and $N < M$ [*Guo et al.*, 2008].

5. Conclusions

In this paper, we have presented a nonlinear resonant mechanism between an oblique whistler wave and electrons, satisfying the resonant condition $\omega - k_\parallel v_\parallel = \Omega_e/2$, by theoretical analysis and test particle simulations. Our mechanism works in a homogeneous plasma with a uniform background magnetic field and may explain the frequency gap at $0.5\Omega_e$ frequently observed in the power spectra of magnetospheric chorus. Furthermore, similar nonlinear resonances may explain the frequency gaps at $0.3\Omega_e$ and $0.6\Omega_e$ in chorus observations recently reported by *Macusova et al.* [2014] and as shown in Figure 1. This mechanism provides a complementary element to existing theories on banded chorus. The detailed theoretical analysis (section 2) will be presented in a separate paper later. The ability of this nonlinear mechanism to explain frequency gaps in chorus emissions needs to be further investigated in a self-consistent way (e.g., via particle-in-cell simulations) to address the dependence of damping rates on various plasma and wave parameters.

Acknowledgments

The authors acknowledge William Kurth, George Hospodarsky, Craig Kletzing, and the Van Allen Probes EMFISIS team for providing wave data. The data are available on the EMFISIS website (https://emfisis.physics.uiowa.edu/data/index). This research was supported in part by the National Aeronautics and Space Administration and by the Laboratory Directed Research and Development program of Los Alamos National Laboratory.

The Editor thanks two anonymous reviewers for their assistance in evaluating this paper.

References

Bell, T. F., U. S. Inan, N. Haque, and J. S. Pickett (2009), Source regions of banded chorus, *Geophys. Res. Lett.*, *36*, L11101, doi:10.1029/2009GL037629.

Carpenter, D. L., and R. R. Anderson (1992), An ISEE/whistler model of equatorial electron density in the magnetosphere, *J. Geophys. Res.*, *97*, 1097–1108.

Chen, L., Z. Lin, and R. White (2001), On resonant heating below the cyclotron frequency, *Phys. Plasmas*, *8* (11), 4713–4716, doi:10.1063/1.1406939.

Dong, C., and N. Singh (2013), Ion pseudoheating by low-frequency Alfvén waves revisited, *Phys. Plasmas*, *20*(1), 12,121.

Fu, X., et al. (2014), Whistler anisotropy instabilities as the source of banded chorus: Van Allen Probes observations and particle-in-cell simulations, *J. Geophys. Res. Space Physics*, *119*, 8288–8298, doi:10.1002/2014JA020364.

Gary, S. P., Y. Kazimura, H. Li, and J.-I. Sakai (2000), Simulations of electron/electron instabilities: Electromagnetic fluctuations, *Phys. Plasmas*, *7*(2), 448–456, doi:10.1063/1.873829.

Gary, S. P., K. Liu, and D. Winske (2011), Whistler anisotropy instability at low electron β: Particle-in-cell simulations, *Phys. Plasmas*, *18* (8), 82,902, doi:10.1063/1.3610378.

Guo, Z., C. Crabtree, and L. Chen (2008), Theory of charged particle heating by low-frequency Alfvén waves, *Phys. Plasmas*, *15*(3), 32,311, doi:10.1063/1.2899326.

Hospodarsky, G. B., T. F. Averkamp, W. S. Kurth, D. a. Gurnett, J. D. Menietti, O. Santolik, and M. K. Dougherty (2008), Observations of chorus at Saturn using the Cassini Radio and Plasma Wave Science instrument, *J. Geophys. Res.*, *113*, A12206, doi:10.1029/2008JA013237.

José, J. V., and E. J. Saletan (1998), *Classical Dynamics: A Contemporary Approach*, Cambridge Univ. Press, Cambridge, U. K.

Kennel, C. F., and F. Engelmann (1966), Velocity space diffusion from weak plasma turbulence in a magnetic field, *Phys. Fluids*, *9*(12), 2377–2388, doi:10.1063/1.1761629.

Li, W., et al. (2013), Characteristics of the Poynting flux and wave normal vectors of whistler-mode waves observed on THEMIS, *J. Geophys. Res. Space Physics*, *118*, 1461–1471, doi:10.1002/jgra.50176.

Liu, K., S. P. Gary, and D. Winske (2011), Excitation of banded whistler waves in the magnetosphere, *Geophys. Res. Lett.*, *38*, L14108, doi:10.1029/2011GL048375.

Lu, Q., and L. Chen (2009), Ion heating by a spectrum of obliquely propagating low-frequency Alfvén waves, *Astrophys. J.*, *704*, 743–749, doi:10.1088/0004-637X/704/1/743.

Macusova, E., O. Santolik, N. Cornilleau-Wehrlin, J. S. Pickett, and D. A. Gurnett (2014), Multi-banded structure of chorus-like emission, in *31st URSI General Assembly and Scientific Symposium (URSI GASS)*, pp. 1–4, IEEE, Beijing, China.

Meredith, N. P., R. B. Horne, A. Sicard-Piet, D. Boscher, K. H. Yearby, W. Li, and R. M. Thorne (2012), Global model of lower band and upper band chorus from multiple satellite observations, *J. Geophys. Res.*, *117*, A10225, doi:10.1029/2012JA017978.

Omura, Y., M. Hikishima, Y. Katoh, D. Summers, and S. Yagitani (2009), Nonlinear mechanisms of lower-band and upper-band VLF chorus emissions in the magnetosphere, *J. Geophys. Res.*, *114*, A07217, doi:10.1029/2009JA014206.

Santolík, O., C. A. Kletzing, W. S. Kurth, G. B. Hospodarsky, and S. R. Bounds (2014), Fine structure of large amplitude chorus wave packets, *Geophys. Res. Lett.*, *41*(2), 293–299, doi:10.1002/2013GL058889.

Sazhin, S. S., and M. Hayakawa (1992), Magnetospheric chorus emissions: A review, *Planet. Space Sci.*, *40*(5), 681–697.

Schriver, D., et al. (2010), Generation of whistler mode emissions in the inner magnetosphere: An event study, *J. Geophys. Res.*, *115*, A00F17, doi:10.1029/2009JA014932.

Stix, T. H. (1992), *Waves in Plasmas*, Springer-Verlag, New York.

Thorne, R. M. (2010), Radiation belt dynamics: The importance of wave-particle interactions, *Geophys. Res. Lett.*, *37*, L22107, doi:10.1029/2010GL044990.

Thorne, R. M., et al. (2013), Rapid local acceleration of relativistic radiation-belt electrons by magnetospheric chorus, *Nature*, *504*(7480), 411–414, doi:10.1038/nature12889.